Applied Surface Science 292 (2014) 777–781

Contents lists available at ScienceDirect

Applied Surface Science

journal homepage: www.elsevier.com/locate/apsusc

Investigation of static and dynamic wetting transitions of UV responsive tunable wetting surfaces

Reeta Pant, Subhash Singha, Aritra Bandyopadhyay [1], Krishnacharya Khare *

Department of Physics, Indian Institute of Technology Kanpur, Kanpur 208016, India

ARTICLE INFO

Article history:
Received 21 October 2013
Received in revised form 4 December 2013
Accepted 8 December 2013
Available online 17 December 2013

Keywords:
Tunable wetting
Surface modification
Superhydrophobic
Titania
Photo-responsive

ABSTRACT

Ultraviolet (UV) radiation responsive surfaces, with tunable wetting properties, are fabricated by spin casting polystyrene/titania nanocomposite dispersion in tetrahydrofuran on silicon substrates. The prepared samples are found hydrophilic due to the presence of the water miscible solvent. Upon annealing, as the solvent evaporates, samples become superhydrophobic due to presence of hydrophobic polystyrene and formation of nano and micro scale surface roughness due to titania nanoparticles. Effect of different annealing temperatures and time on resulting wettability is investigated. Photocatalytic property of titania is exploited to make transition from superhydrophobic to hydrophilic state upon UV exposure. Subsequently, upon annealing again at elevated temperatures for sufficient time, the UV exposed hydrophilic samples recover their superhydrophobicity showing transition from hydrophilic to superhydrophobic state. Detailed static and dynamic study of these reversible transitions, between superhydrophobic and hydrophilic states, due to UV exposure and annealing is presented in this article.

1. Introduction

Smart surfaces with tunable wetting properties have recently gained considerable attention from fundamental as well as application point of view. Various research groups have shown different applications of such tunable wetting surfaces in areas including microfluidic devices, biosensors, drug delivery, bio-separation, anti-adhesive coatings, self-cleaning surfaces etc [1–6]. Significant amount of work has been done in recent time to fabricate such smart surfaces with tunable wettability based on different external stimulus e.g. electric field, temperature, light, pH, humidity, mechanical strain, gas, redox electrochemistry etc [7–14]. Among these techniques, the light (specifically UV radiation) responsive approach has received special attention because of its simplicity in fabrication as well as the cost effectiveness. UV responsive tunable wetting surfaces are used in wide range of applications as there is no specific requirement for substrates and liquids which is essentially required for most other responsive techniques.

It has been well understood that the wettability of a surface can be tuned either by controlling its surface chemistry or surface topography or combination of both [15–17]. On homogeneous (chemically as well as topographically) surfaces, the equilibrium contact angle (θ) are given by the Young's equation [18]. Whereas on rough and/or heterogeneous surfaces, the apparent contact angle can be described by the Wenzel or the Cassie–Baxter model depending upon the heterogeneity [19,20]. Many research groups have successfully attempted to fabricate superhydrophobic surfaces (with water contact angle >150°) exploiting combination of chemical and topographical heterogeneities [21–24]. To fabricate smart surfaces with tunable wetting property, one needs to use a coating that responds to a particular external stimulus. Various research groups have fabricated UV responsive tunable wetting surfaces based on different transition metal oxides, such as ZnO, TiO_2, WO_3, SnO_2, Fe_2O_3, and V_2O_5 [25–28]. These transition metal oxides exhibit photoinduced hydrophilicity when exposed to UV radiation. Among these transition metal oxides, titania (TiO_2) is an important material which is widely used in many industrial applications including photo catalysis, photovoltaic devices, photo splitting of water, sunscreens etc. Due to photo catalytic property of titania, it is widely used as light-induced hydrophilic surfaces [5,29,30]. It has been demonstrated with fourier transform infrared spectroscopy (FTIR) and X-ray photoelectron spectroscopy (XPS) studies that, upon UV exposure of TiO_2 surfaces, the equilibrium Ti^{4+} ions are converted into Ti^{3+} defect states accompanying oxygen vacancy [5,31,32]. Therefore, Ti^{3+} defect sites have the affinity to chemisorb water molecules making the surface hydrophilic. The photo catalytic phenomenon of titania upon UV exposure can be summarized by following reactions [33]:

$$TiO_2 + h\nu \rightarrow h^+_{\text{valenceband}} + e^-_{\text{conductionband}}$$

* Corresponding author. Tel.: +915122597968; fax: +915122590914.
E-mail address: kcharya@iitk.ac.in (K. Khare).
[1] Saha Institute of Nuclear Physics, Kolkata - 700064, India.

0169-4332/$ – see front matter © 2013 Elsevier B.V. All rights reserved.
http://dx.doi.org/10.1016/j.apsusc.2013.12.049

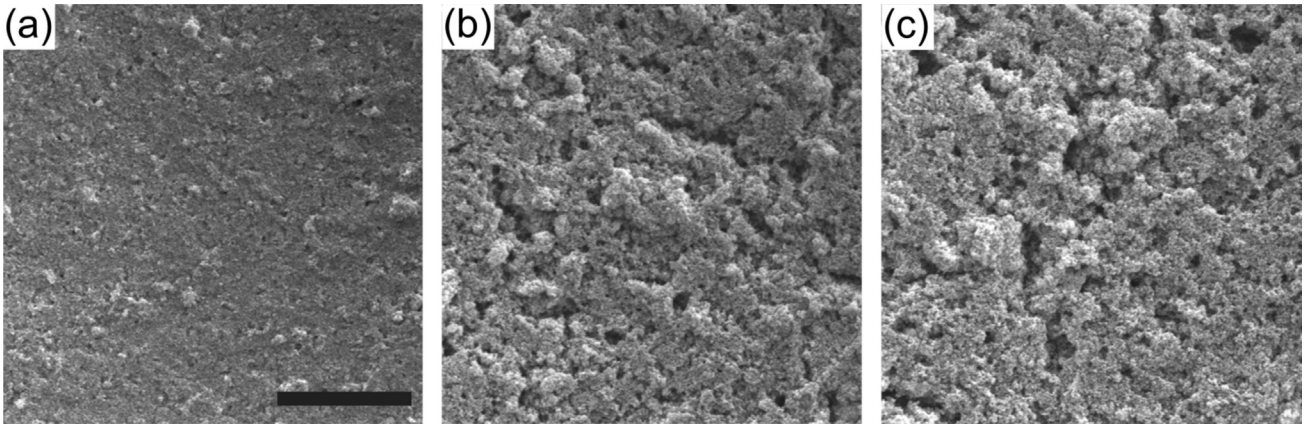

Fig. 1. SEM micrographs of PS/TiO_2 nanocomposite films of (a) as prepared sample, (b) sample annealed at 180 °C, and (c) sample exposed to UV radiation for 150 min. Scale bar in the image correspond to 5 μm and is same for all three images.

$$e^-_{\text{conductionband}} + Ti^{4+} \rightarrow Ti^{3+}_{\text{trappedelectron}}$$

$$h^+_{\text{valenceband}} + O^{2-} \rightarrow O^-_{\text{trappedhole}}$$

$$4h^+_{\text{valenceband}} + 2O^{2-} \rightarrow O_2$$

It has also been reported that annealing titania at temperatures higher than 250 °C causes hydrophilicity due to desorption of surface oxygen, producing oxygen vacancies. One missing oxygen atom at the bridging-O site leaves two subsurface Ti^{3+} sites exposed thus making the surface hydrophilic [34].

Inspired by the photo catalytic property of titania, many researchers have fabricated nanostructured titania films to exhibit UV tunable superhydrophobic behavior [25,31,32,35]. Due to the nanostructuring of titania films, these methods are neither very convenient nor cost effective. Alternatively, Hou et al. demonstrated mixing of titania nanoparticles with a hydrophobic polymer providing similar results with much simpler fabrication recipe [7]. Similar phenomenon may also be observed when polystyrene or some other hydrophobic polymer is mixed with the above mentioned metal oxides. The combination of hydrophobic polystyrene and photo catalytic titania nanoparticles provide easy fabrication recipe without any need of nanostructuring or nanopatterning and also better control over reversible switching of wettability. They demonstrated tunable wettability upon UV exposure and subsequent annealing, but their study lacked detailed investigation of the wetting transitions. For any tunable wetting surfaces, knowledge of static and dynamic wetting transitions is important as it provides characteristic information of the surface as well as its dynamic tuning [36–39]. In this paper, we present detailed analysis of static and dynamics of both wetting transitions (superhydrophobic to hydrophilic and vice versa) for many repeat cycles.

2. Experimental section

Single side polished silicon (Si) wafers cut into square pieces (2 cm × 2 cm) were used as substrates. The substrates were thoroughly cleaned by ultrasonicating in ethanol, acetone, and toluene followed by plasma cleaning (Harrick Plasma, USA). 2 wt.% polystyrene (PS) (Polymer Standards Service Germany, 100 kg/mol) was dissolved in tetrahydrofuran (THF) and ultrasonicated for 10 min to prepare homogeneous solution. 5 wt.% titania nanoparticles (mean diameter ~21 nm, Aldrich) were mixed in the prepared PS/THF solution and the mixture was ultrasonicated for 1 h to prepare a good dispersion. The PS/THF/TiO_2 dispersion was then spin coated (RPM 1000, acceleration time 25 s, spin time 90 s) on pre-cleaned Si substrates. The resulting film thickness was found to be 35(±4)μm. Films with different thickness were prepared by varying the concentration of the dispersion and changing the spin coating parameters These samples were subsequently annealed at different temperatures for different time and their resulting surface roughness and wettability were characterized as a function of annealing temperature and time. Surface roughness measurements were carried out by an atomic force microscope (AFM) (PicoSPM, Non-contact mode, Molecular Imaging Corporation) over 3 μm × 3 μm surface area. Wettability measurements were carried out using an optical contact angle goniometer (OCA35, Dataphysics Germany) using sessile drop (of de-ionized water) method with fixed drop volume of 2 μl. Later the annealed samples were exposed to UV radiation (wavelength 254 nm, power output 350 μW/cm^2) and their wettability and surface roughness were characterized as a function of increasing UV exposure time. Since the bulk band gap of the TiO_2 is 3.2 eV, and as the crystallite size decreases, the band gap increases reaching up to 3.4 eV for crystallite size of 20 nm [40]. We initially exposed the PS/TiO_2 nanocomposite films to 364 nm UV radiation, but failed to see any wettability change. Subsequently we exposed with 254 nm UV radiation which gave the desired result. After UV exposure, samples were again annealed at different temperatures for different time to study their superhydrophobic recovery. This whole analysis was repeated for many cycles to study the reversible wetting transition and possible contact angle hysteresis.

3. Results and discussion

After spin casting PS/TiO_2/THF dispersion on silicon substrates, the as prepared samples were found hydrophilic (water contact angle $\theta \sim 42\ (\pm 2)^\circ$) due to presence of the solvent THF in thin films which is water miscible. Samples with different film thicknesses didn't show any significant difference in the resulting wetting behavior due to the fact that wetting is a surface phenomenon and depends only upon chemistry and topography of the top surface. Fig. 1(a) shows the scanning electron microscope (SEM) image of an as prepared sample which had rms roughness of 95 nm as analyzed by the AFM. This surface roughness could be mainly due to agglomerated titania nanoparticles at the surface.

As prepared samples were annealed at different temperatures for different time and their surface roughness as well as surface wettability were characterized. Fig. 2(a) shows the plot of rms surface roughness (left *Y*-axis) of an as prepared sample as a function of annealing temperature as well as the corresponding water contact

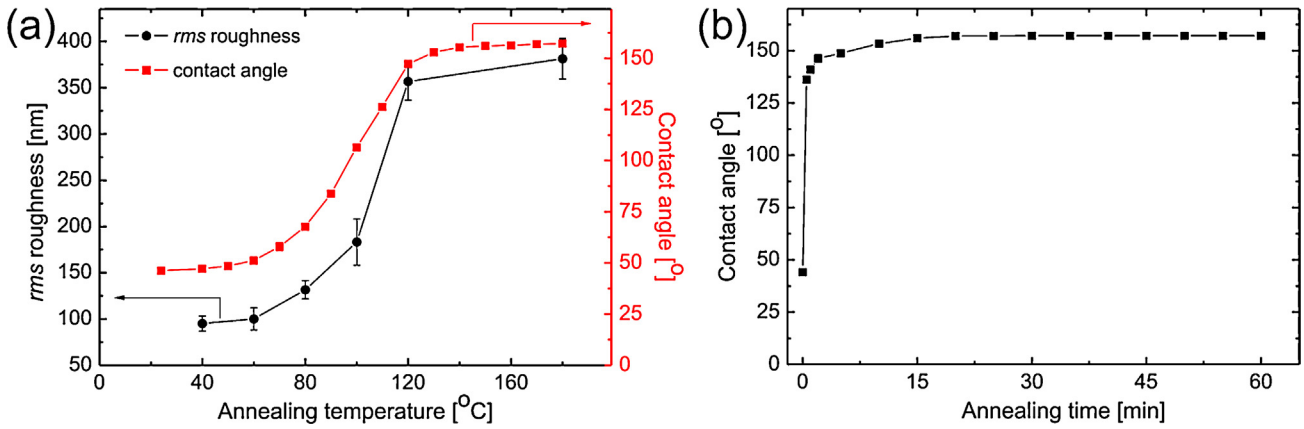

Fig. 2. (a) rms surface roughness and resulting contact angle of PS/TiO_2 nanocomposite samples as a function of annealing temperature. (b) Contact angle variation of samples annealed at 180 °C for different time.

angles (right *Y*-axis). It is clear from the graph that as the annealing temperature increases, the surface roughness also increases thus increasing the apparent contact angle. Initially, till temperature close to the boiling point of THF (66 °C), the solvent THF starts to boil and molecular reordering takes place at the surface which increases the surface roughness. As a result, the apparent contact angle is also increased. We calculated the apparent contact angle via Wenzel model for smaller surface roughness (typically <250 nm, obtained from Fig. 2(a)) and found the apparent contact angle values in agreement with experimental observations. At higher temperatures (>100 °C), THF vapors trapped underneath the surface starts escaping, creating big micron size cracks at the surface as confirmed by SEM images. The phenomenon of cracks formation due to solvent evaporation has been demonstrated for drying soils and clay [41,42]. Therefore the sudden increase in the surface roughness is observed.

For temperatures more than 110 °C, PS undergoes glass transition ($T_g \sim 110$ °C) and TiO_2 nanoparticles agglomerates more to further increase the roughness slightly. The rms roughness of samples annealed at 180 °C was found as large as 380 nm. Fig. 1(b) shows the SEM image of a sample annealed at 180 °C for 60 min. The image clearly indicates presence of dual scale roughness: micro-scale roughness due to cracks and nano-scale roughness due to agglomerated TiO_2 nanoparticles. Due to the dual scale roughness, the sample showed superhydrophobic behavior with water contact angle as high as 157(±2)°. In this case also we calculated the apparent contact angle via Cassie–Baxter model and found the contact angle value in agreement with the experimental one. We found that below rms surface roughness of 350 nm, liquid drops were in Wenzel state whereas above it they were in Cassie–Baxter state. We also studied the effect of annealing time (dynamics) on the resulting wettability. For this, the as prepared samples were annealed at 180 °C for different times and the result is shown in Fig. 2(b).

It is clear from the plot that the samples became superhydrophobic in first few minutes of annealing. This is due to the fact that THF boils and evaporates very quickly and the dual scale roughness is created in first few minutes of the annealing showing superhydrophobic behavior. Fig. 3 shows AFM images of as prepared and annealed samples which clearly shows increase in roughness which is the main cause of the superhydrophobicity.

The superhydrophobic samples, obtained by annealing the as prepared samples at 180 °C for 60 min, were exposed to UV radiation and their wettability was analyzed as a function of UV exposure time. As discussed earlier, UV radiation induces photo catalytic decomposition in TiO_2.

The equilibrium electronic state of Ti in TiO_2 is Ti^{4+} which is converted into Ti^{3+} upon UV exposure. These Ti^{3+} states are defects sites and acts as thermodynamically favorable centers to accommodate water molecules thus making the surface hydrophilic. Fig. 4 shows the plot of apparent contact angle of the superhydrophobic samples annealed at 180 °C for 60 min upon UV exposure. It is clear from the plot that the rate of decrement of contact angle is smaller in the beginning but increases with increase in UV exposure time. This is due to the fact that larger number of Ti^{3+} defect states is produced with increasing UV exposure time making the surface hydrophilic at faster rate. Samples exposed to UV for about 135 min become completely hydrophilic with complete spreading of water drops ($\theta \sim 0°$). We confirmed with AFM measurements that the surface roughness of the samples was not affected by UV exposure. The surface roughness of all UV exposed samples was found about 380 nm. So the decrease in contact angle can solely be

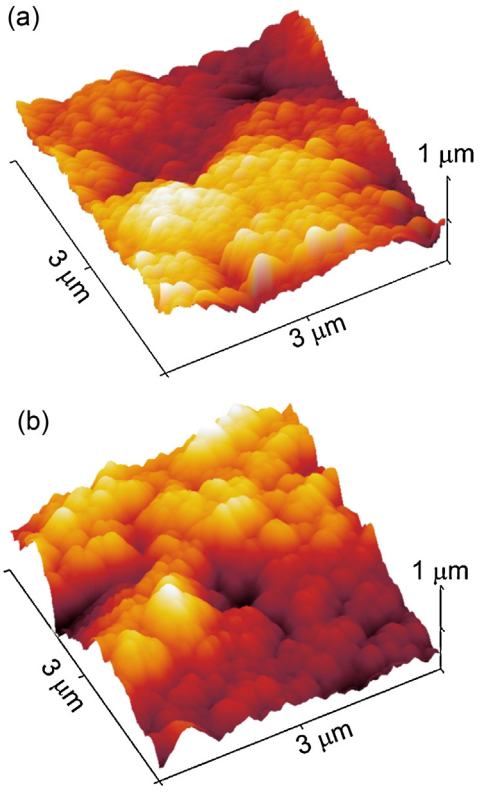

Fig. 3. AFM micrographs of (a) as prepared and (b) annealed at 180 °C samples clearly indicating the increase in roughness after annealing.

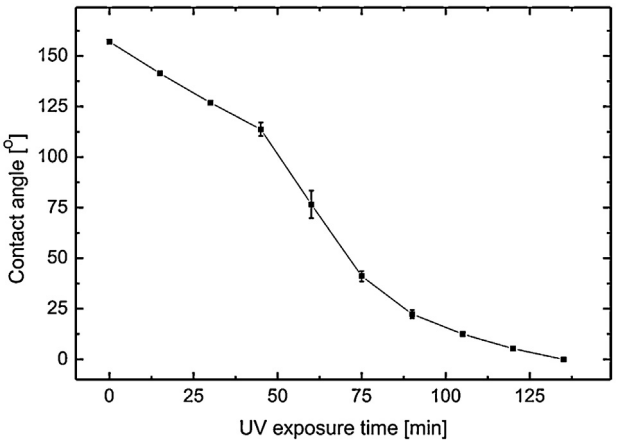

Fig. 4. Variation of water contact angle of annealed superhydrophobic samples as a function of UV exposure time.

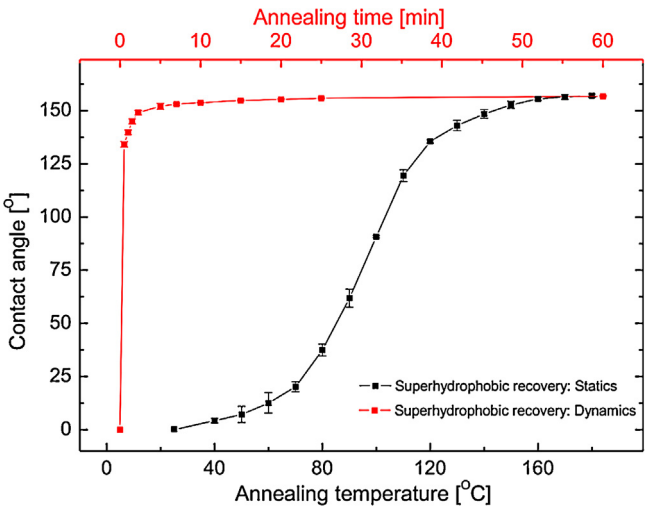

Fig. 5. Static and dynamic study of superhydrophobic recovery of UV exposed samples. Change of contact angle was measured with changing annealing temperature (bottom *X*-axis) and annealing time (top *X*-axis).

attributed to the change in electronic state (from equilibrium Ti^{4+} to defect Ti^{3+}) of titanium atoms at the surface.

Subsequent to the UV exposure, the samples were annealed again and the static and dynamic analysis of their superhydrophobic recovery was performed. Static superhydrophobic recovery experiments were done by annealing the UV exposed hydrophilic samples to different temperatures, starting from room temperature till 180 °C, for 60 min whereas the dynamics experiments were done by annealing the samples at 180 °C for different times. Fig. 5 shows the plot of contact angle as a function of annealing temperature (bottom *X*-axis) and annealing time (top *X*-axis). As the annealing temperature increases, the defect Ti^{3+} ions gain energy to go back to their equilibrium Ti^{4+} states and the samples slowly recover their superhydrophobicity. Here one should keep in mind that the phenomenon for 1st cycle of annealing (cf. Fig. 2) is completely different from the 2nd (and so forth) cycle of annealing.

During the 2nd cycle of annealing, the surface roughness does not change at all and the change in electronic states of titanium ions (from defect Ti^{3+} to equilibrium Ti^{4+}) is solely responsible for superhydrophobic recovery. Presence of polystyrene enhances the superhydrophobic recovery during the annealing because the adsorbed hydroxyl groups at the defect Ti^{3+} sites are replaced by oxygen atoms. The dynamics analysis also shows that the superhydrophobic recovery occurs in first few minutes very similar as in the case of 1st cycle annealing. So even though the mechanism of 1st cycle and 2nd cycle heating is entirely different, qualitatively the contact angle behavior looks similar. Subsequently the samples were further exposed to UV followed by annealing for several cycles. Fig. 6 shows optical contact angle images, obtained from a contact angle goniometer, for (a) as prepared sample with $\theta = 40°$, (b) annealed sample at 180 °C for 60 min with $\theta = 157°$, and (c) UV exposed sample with $\theta = 0°$ showing reversible transition from superhydrophobic to hydrophilic. Fig. 6(d) shows plot of contact angles upon annealing the samples at 180 °C and UV exposure for three cycles. This experiment was repeated over 50 cycles and no

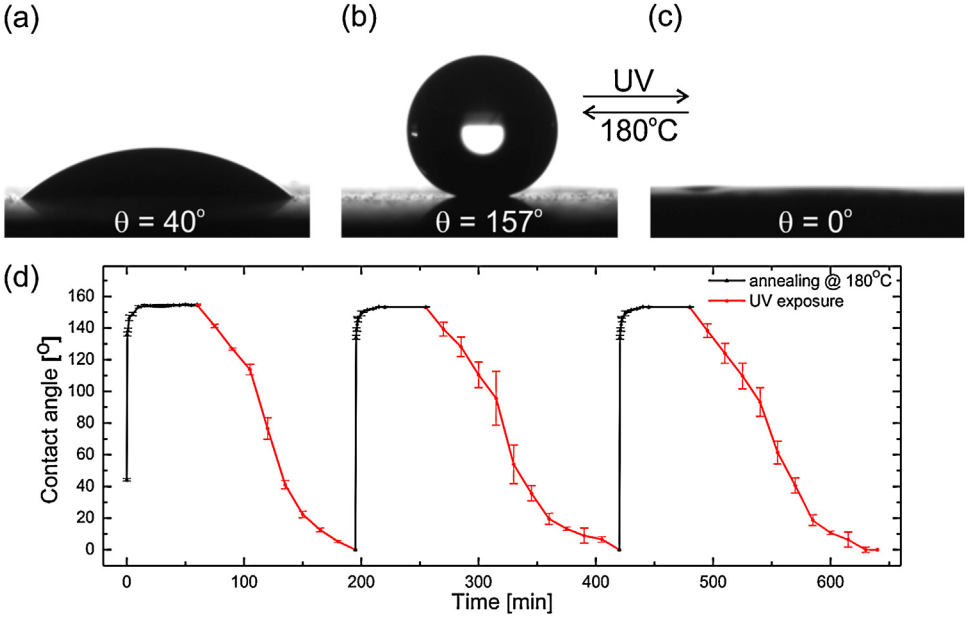

Fig. 6. Optical contact angle images of a water droplet on (a) as prepared, (b) annealed, and (c) UV exposed samples. A reversible transition between superhydrophobic and hydrophilic states can be obtained by annealing at 180 °C and UV exposure for 135 min. (d) Dynamics of contact angle variation with UV exposure and annealing for three transition cycles.

contact angle hysteresis was observed indicating the good stability of the nanocomposite film. Thus PS/TiO_2 nanocomposite films can be used as UV responsive tunable wetting surfaces without the loss of their characteristics over large time period.

4. Conclusion

Polystyrene/titania nanocomposite samples were prepared by spin coating PS/TiO_2/THF dispersion. The as prepared samples were annealed at different temperatures for different time to analyze the static (with temperature) and dynamic (with time) wetting transitions from hydrophilic to super hydrophobic states. In this 1st cycle of annealing, samples became superhydrophobic due to formation of dual scale roughness (nano scale due to TiO_2 nanoparticles and micro scale due to cracks created during THF vapors escape). Surface roughness of these annealed samples analyzed by an AFM confirmed that it increased with annealing temperature. The apparent contact angles of the annealed samples were also calculated theoretically using Wenzel and Cassie–Baxter model depending upon the surface roughness. These superhydrophobic samples were exposed to UV radiation for different times and it was found that the samples slowly became completely hydrophilic. This was due to the fact that upon UV exposure, the equilibrium titanium ions in TiO_2, which were in Ti^{4+} states went into Ti^{3+} states which act as defect states and have affinity towards water molecules. We also confirmed that the surface roughness for UV exposed samples remains same during complete UV exposure cycle. Subsequently the UV exposed hydrophilic samples were annealed again at 180 °C for 60 min and they again became superhydrophobic with almost zero hysteresis. We also confirmed that in this case the surface roughness again remains constant and the superhydrophobic recovery is solely due to conversion of Ti^{3+} defect states into Ti^{4+} equilibrium states. This reversible transition between superhydrophobic to complete hydrophilic states was performed for more than 50 cycles and no hysteresis was observed.

Acknowledgement

This research work was supported by BRNS (DAE) Young Scientist Research Award and DST, New Delhi through its Unit of Excellence on Soft Nanofabrication at IIT Kanpur.

References

[1] R. Blossey, Self-cleaning surfaces—virtual realities, Nat. Mater. 2 (2003) 301–306.
[2] S.C. D'Andrea, A.Y. Fadeev, Wettability changes induced by biochemical surface reactions, Langmuir 22 (2006) 3962–3963.
[3] A. Honglawan, H. Ni, D.D. Weissmanb, S. Yang, Synthesis of random copolymer based pH-responsive nanoparticles as drug carriers for Cancer therapeutics, Polym. Chem. 4 (2013) 3667–3675.
[4] J. Lahann, S. Mitragotri, T.N. Tran, H. Kaido, J. Sundaram, I.S. Choi, S. Hoffer, G.A. Somorjai, R. Langer, A reversibly switching surface, Science 299 (2003) 371–374.
[5] R. Wang, K. Hashimoto, A. Fujishima, M. Chikuni, E. Kojima, A. Kitamura, M. Shimohigoshi, T. Watanabe, Light-induced amphiphilic surfaces, Nature 388 (1997) 431–432.
[6] B. Zhao, J.S. Moore, D.J. Beebe, Surface-directed liquid flow inside micro channels, Science 291 (2001) 1023–1026.
[7] W. Hou, Q. Wang, UV-driven reversible switching of a polystyrene/titania nanocomposite coating between superhydrophobicity and super hydrophilicity, Langmuir 25 (2009) 6875–6879.
[8] T.N. Krupenkin, J.A. Taylor, E.N. Wang, P. Kolodner, M. Hodes, T.R. Salamon, Reversible wetting-dewetting transitions on electrically tunable superhydrophobic nanostructured surfaces, Langmuir 23 (2007) 9128–9133.
[9] T. Sun, G. Wang, L. Feng, B. Liu, Y. Ma, L. Jiang, D. Zhu, Reversible switching between super hydrophilicity and superhydrophobicity, Angew. Chem. Int. Ed. 43 (2004) 357–360.
[10] L. Xu, W. Chen, A. Mulchandani, Y. Yan, Reversible conversion of conducting polymer films from superhydrophobic to super hydrophilic, Angew. Chem. Int. Ed. 44 (2005) 6009–6012.
[11] Y.H. Yeong, A. Steele, E. Loth, I. Bayer, G.D. Combarieu, C. Lakeman, Temperature, Humidity effects on superhydrophobicity of nanocomposite coatings, Appl. Phys. Lett. 100 (2012) 053112–053114.
[12] X. Yu, Z. Wang, Y. Jiang, F. Shi, X. Zhang, Reversible pH-responsive surfaces: from superhydrophobicity to super hydrophilicity, Adv. Mater. 17 (2005) 1289–1293.
[13] J. Zhang, X. Lu, W. Huang, Y. Han, Reversible superhydrophobicity to superhydrophilicity transition by extending and unloading an elastic polyamide film, Macromol. Rapid Commun. 26 (2005) 477–480.
[14] Y. Zhu, J. Li, H. He, M. Wan, L. Jiang, Reversible wettability switching of polyaniline-coated fabric, triggered by ammonia gas, Macromol. Rapid Commun. 28 (2007) 2230–2236.
[15] L. Feng, S. Li, Y. Li, H. Li, L. Zhang, J. Zhai, Y. Song, B. Liu, L. Jiang, D. Zhu, Super-hydrophobic surfaces from natural to artificial, Adv. Mater. 14 (2012) 1857–1860.
[16] K.K.S. Lau, J. Bico, K.B.K. Teo, M. Chhowalla, G.A.J. Amaratunga, W.I. Milne, G.H. McKinley, K.K. Gleason, Superhydrophobic carbon nanotube forests, Nano Lett. 3 (2003) 1701–1705.
[17] X.Y. Ling, I.Y. Phang, G.J. Vancso, J. Huskens, D.N. Reinhoudt, Stable and transparent superhydrophobic nanoparticle films, Langmuir 25 (2006) 3260–3263.
[18] T. Young, An essay on the cohesion of fluids, Phil. Trans. R. Soc. Lond. 95 (1805) 65–87.
[19] A.B.D. Cassie, S. Baxter, Wettability of porous surfaces, Trans. Faraday Soc. 40 (1944) 546–551.
[20] R.N. Wenzel, Resistance of solid surfaces to wetting by water, Ind. Eng. Chem. 28 (1936) 988–994.
[21] H.Y. Erbil, A.L. Demirel, Y. Avci, O. Mert, Transformation of a simple plastic into a superhydrophobic surface, Science 299 (2003) 1377–1380.
[22] H. Li, X. Wang, Y. Song, Y. Liu, Q. Li, L. Jiang, D. Zhu, Super-amphiphobic aligned carbon nanotube films, Angew. Chem. Int. Ed. 40 (2001) 1743–1746.
[23] A. Tuteja, W. Choi, M. Ma, J.M. Mabry, S.A. Mazzella, G.C. Rutledge, G.H. McKinley, R.E. Cohen, Designing superoleophobic surfaces, Science 318 (2007) 1618–1622.
[24] L. Zhai, F.C. Cebeci, R.E. Cohen, M.F. Rubner, Stable superhydrophobic coatings from polyelectrolyte multilayers, Nano Lett. 4 (2004) 1349–1353.
[25] X.J. Feng, L. Feng, M.H. Jin, J. Zhai, L. Jiang, D.B. Zhu, Reversible superhydrophobicity to super-hydrophilicity transition of aligned ZnO nanorod films, J. Am. Chem. Soc. 126 (2004) 62–63.
[26] H.S. Lim, D. Kwak, D.Y. Lee, S.G. Lee, K. Cho, UV-driven reversible switching of a rose like vanadium oxide film between superhydrophobicity and super hydrophilicity, J. Am. Chem. Soc. 129 (2007) 4128–4129.
[27] M. Miyauchi, A. Nakajima, T. Watanabe, K. Hashimoto, Photocatalysis, Photo induced hydrophilicity of various metal oxide thin films, Chem. Mater. 14 (2002) 2812–2816.
[28] B. Yan, J. Tao, C. Pang, Z. Zheng, Z. Shen, C.H.A. Huan, T. Yu, Reversible UV-light-induced ultra hydrophobic-to-ultra hydrophilic transition in an an α-Fe_2O_3 nanoflakes film, Langmuir 24 (2008) 10569–10571.
[29] M.A. Henderson, An HREELS and TPD study of water on TiO_2(1 1 0): the extent of molecular versus dissociative adsorption, Surf. Sci. 355 (1996) 151–166.
[30] M.B. Hugenschmidt, L. Gamble, C.T. Campbell, The interaction of H_2O with a TiO_2(1 1 0) surface, Surf. Sci. 302 (1994) 329–340.
[31] T. Watanabe, A. Nakajima, R. Wang, M. Minabe, S. Koizumi, A. Fujishima, K. Hashimoto, Photocatalytic activity and photo induced hydrophilicity of titanium dioxide coated glass, Thin Solid Films 351 (1999) 260–263.
[32] X. Zhang, M. Jin, Z. Liu, S. Nishimoto, H. Saito, T. Murakami, A. Fujishima, Preparation and photo catalytic wettability conversion of TiO_2-based super hydrophobic surfaces, Langmuir 22 (2006) 9477–9479.
[33] L.B. Xiong, J.L. Li, B. Yang, Y. Yu, Ti^{3+} in the surface of titanium dioxide: generation, properties and photo catalytic application, J. Nano Mat. 2012 (2011) 1–13.
[34] G. Lu, A. Linsebigler, J.T. Yates Jr., Ti^{3+} defect sites on TiO_2(1 1 0): production and chemical detection of active sites, J. Phys. Chem. 98 (1994) 11733–11738.
[35] X. Zhang, M. Jin, Z. Liu, D.A. Tryk, S. Nishimoto, T. Murakami, A. Fujishima, Superhydrophobic TiO_2 surfaces: preparation, photo catalytic wettability conversion, and superhydrophobic-super hydrophilic patterning, J. Phys. Chem. C 111 (2007) 14521–14529.
[36] P.G. de Gennes, Wetting: statics and dynamics, Rev. Mod. Phys. 57 (1985) 827–863.
[37] H.S. Lim, S.G. Lee, D.H. Lee, D.Y. Lee, S. Lee, K. Cho, Superhydrophobic to super hydrophilic wetting transition with programmable ion-pairing interaction, Adv. Mater. 20 (2008) 4438–4441.
[38] X. Liu, Q. Ye, X. Song, Y. Zhu, X. Cao, Y. Liang, F. Zhou, Responsive wetting transition on superhydrophobic surfaces with sparsely grafted polymer brushes, Soft Matter 7 (2011) 515–523.
[39] J.V.I. Timonen, M. Latikka, L. Leibler, R.H.A. Ras, O. Ikkala, Switchable static and dynamic self-assembly of magnetic droplets on superhydrophobic surfaces, Science 341 (2013) 253–257.
[40] K.M. Reddy, S.V. Manorama, A.R. Reddy, Band gap studies on anatase titanium dioxide nanoparticles, Mater. Chem. Phys. 78 (2002) 239–245.
[41] C.J. Miller, H. Mi, N. Yesiller, Experimental analysis of desiccation crack propagation in clay liners, J. Am. Water Resour. Assoc. 34 (1998) 677–686.
[42] J.H. Wu, S. Yang, Study on crack spacing and width of expansive soil due to evaporation, Adv. Mater. Res. (Durnten-Zurich, Switz.) 690–693 (2013) 728–733.